Mid-ocean ridge or marginal basin origin of the East Taiwan Ophiolite: chemical and isotopic evidence

Bor-ming Jahn

CAESS-CNRS and Université de Rennes, Institut de Géologie, F-35042 Rennes Cedex, France

Abstract. The East Taiwan Ophiolite (ETO) occurs as allochthonous fragments embedded in the Plio-Pleistocene Lichi Mélange in the Coastal Range of eastern Taiwan. It is probably the youngest among the known ophiolitic complexes of the world. The overall geochemical and isotopic characteristics of the representative rock types are very "oceanic" and strongly argue for a mid-ocean or marginal basin origin of the ETO. The best criteria include: (1) major element compositions; (2) REE distribution patterns; (3) Nd isotopic ratios (some have $\varepsilon_{Nd} \geq +12$); (4) Pb isotopic ratios; and (5) the presence and nature of the red shale. This conclusion is supported by previous studies of metamorphic evolution of the ETO.

The occurrence of both N- and P-type basalts in the ETO is firmly recognized for the first time by their REE distribution patterns. Neither type of basalt could be derived by fractional crystallisation from the other, nor by various degrees of partial melting from a common mantle source. Consequently, the genesis of basaltic magmas of the ETO has probably involved melting and mixing of a highly depleted asthenosphere and an enriched plume-type or hot-spot source.

Because of the young age of formation (about 15 Ma) and the very recent tectonosedimentary emplacement (olistostromal origin) through arc-continent collision (about 4–5 Ma), the ETO was most likely generated in the spreading center of a small ocean or marginal basin (the South China Sea).

Introduction

Taiwan is situated at the eastern margin of the Eurasian continental plate and is undergoing spectacular deformation, metamorphism, uplift and erosion as a result of active collision between the continental plate margin and an island arc of the Philippine Sea plate. The northern part of this island arc (the Luzon Arc) now forms the bulk of the Coastal Range of eastern Taiwan (Ho 1982).

The East Taiwan Ophiolite (ETO) occurs as allochthonous fragments dispersed in the Plio-Pleistocene Lichi Mélange in the Coastal Range of eastern Taiwan (Fig. 1). These fragments are distributed roughly along the eastern side of the Longitudinal Valley for about 60 km (Hsu 1956; Ho 1975, 1982; Liou et al. 1977; Page and Suppe 1981). Although the ETO does not show an intact ophiolite stratigraphy, it contains all necessary rock types as defined

in an ideal ophiolite complex, such as, harzburgite, dunite, serpentinite, gabbro, dolerite, pillow basalt, plagiogranite, red shale (red clay), etc. (Juan 1964; Wang 1966; Liou et al. 1977). A schematic stratigraphic relationship has been reconstructed by Liou et al. (1977) and Suppe et al. (1981). The field occurrence of the ophiolite blocks or slabs and the nature of their enclosing Lichi Mélange were previously reported by Hsu (1956, 1976) and Wang (1976), and a detailed account was recently given by Page and Suppe (1981), who considered the Pliocene Lichi Mélange to have an olistostromal origin. In addition to the ophiolitic blocks, the Lichi Mélange also contains detritus of the adjacent calcalkaline terrane (= the Luzon Arc) and some basement rocks and Cenozoic sediments of the Asiatic continental margin.

According to Liou et al. (1977) and Suppe et al. (1981), the original ophiolite stratigraphy consists of a basal plutonic sequence composed of fragments of gabbro, diabase and ultrabasic rocks capped by pelagic red shale and an overlying extrusive sequence of basaltic pillow lavas, volcanic breccias, and some intercalated red shales. The red shales contain no terrigenous debris and very little calcareous components, hence they were thought to be deposited below the calcite compensation depth. Consequently, the basaltic flows were probably formed far from land in water deeper than about 4 km, presumably on old oceanic crust (Liou et al. 1977; Suppe et al. 1981).

Available geochemical data, mainly of major elements and limited trace element and isotopic (Sr, Pb) abundances, have been used to support an origin of the ETO at an oceanic spreading center (Shih et al. 1972; Liou et al. 1977). Based primarily on the occurrence of intercalated red shales in the pillow lava sequence, Suppe et al. (1981) further suggested that the ophiolite was not deposited at a normal oceanic ridge, but rather along a transform or other non-ridge-crest fault. On the other hand, a drastically different interpretation of the same geochemical data was given by V.C. Juan and his coworkers (Juan 1975; Juan et al. 1978, 1980; Chou et al. 1978). In their opinion, the igneous rocks, called the Kuanshan Igneous Complex instead of the ETO, were formed at a subduction zone near the plate boundary now represented by the Longitudinal Valley. In other words, these rocks were formed in an environment similar to island arc setting and were emplaced roughly *in situ* at the present sites.

Since the pioneer work of Pearce and Cann (1973), the use of geochemical diagrams in identifying the paleo-tec-
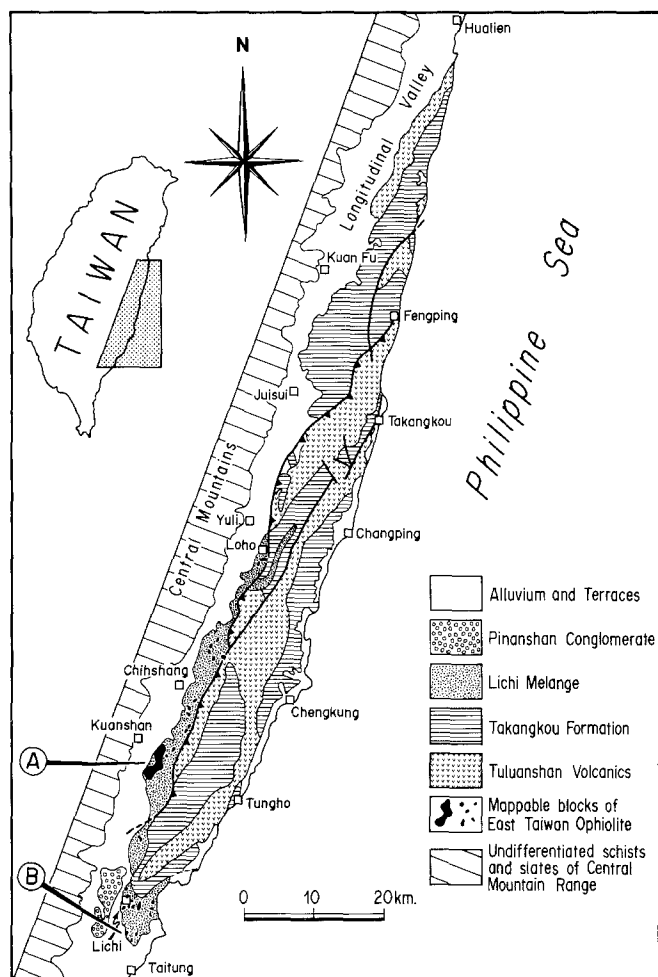
Fig. 1. Geologic map of the Coastal Range of Taiwan (after Ernst and Liou, 1985) and distribution of the ETO blocks. Samples of the present study come from two areas A and B

the Samail Ophiolite (Pearce 1982; Pearce et al. 1981; Moores et al. 1984). Although an island arc origin for ophiolites is gaining support from new observations and geochemical analyses (e.g., Noiret et al. 1981; Gerlach et al. 1981a, Hawkins 1980), there is no doubt that ophiolites may have multiple origins at diverse tectonic settings (Coleman 1977, 1984; Moores 1982). The present work attempts to integrate available geochemical and isotopic data in the hope that the controversial issue on the interpretation of the ETO would be settled with these geochemical signatures even without much consideration of the geological context. It is not my purpose here to discuss petrogenetic processes in detail through the use of trace element and isotopic data. Moreover, it must be emphasized that, although detectable difference may exist in some cases (Tarney et al. 1981; Cohen and O'Nions 1982), there is little distinction in overall geochemical and isotopic characteristics between the basalts formed at mid-ocean ridges (s.s.) and in marginal basins; thus the "mid-ocean ridge" expressed in the title should be considered geochemically synonymous to "spreading ridge of marginal basin". In the case of the East Taiwan Ophiolite, the marginal basin concerned is represented by the South China Sea (Suppe et al. 1981). In terms of the age of formation (about 15 Ma) and the time of emplacement through collisional process (about 4 Ma), the ETO is probably the *youngest* among the known ophiolitic complexes of the world (See Appendix 2 for further age information).

Sampling and analytical methods

Blocks and fragments representing the entire range of ophiolitic rock types are widespread in the Lichi Mélange (Liou et al. 1977). The Lichi Mélange, however, incorporates more abundant sedimentary blocks including sandstone, siltstone, shale, mudstone and minor amounts of limestone and conglomerate. By contrast, some rock types that are well known as blocks in ophiolite-bearing tectonic mélanges are missing here. For example, glaucophane schist and pelagic radiolarian chert that are common in the Franciscan mélange are entirely absent. Also missing are blocks of continental basement rocks such as those in the northern Apennines or central Java (Page and Suppe 1981). Furthermore, a sheeted dike complex is not clearly represented here, perhaps due partly to the limited exposure.

All representative rock types of the ETO have been sampled, although the list may not be complete (see Table 1). The glass fractions of pillow basalts were separated by hand-picking from moderately ground samples; all other whole-rock powder samples were prepared using agate mortars. Except for major element analyses of glass samples done at Centre Oceanographique de Bretagne, Brest, all chemical and isotopic analyses were performed in the laboratories of the Université de Rennes. Major and trace element (except REE) abundances were determined by the XRF method. Na_2O and MgO contents were obtained by the atomic absorption method. The uncertainties for all major elements were estimated at 1 to 5%, and for trace elements ranging from 5 to 20%, depending on individual element.

Rare earth elements (REE) were determined by the isotopic dilution method. A brief description of analytical procedures can be found in Jahn et al. (1980a). Total analytical errors were estimated about 3% for La and Lu, and 2% for other REE. Isotopic data were obtained using the same method described by Jahn et al. (1980b) for Nd, and by Vidal and Clauer (1981) for Pb. The measured Pb isotopic ratios have been adjusted to the certified values given by Catanzaro et al. (1968). Maximum uncertainties for Pb isotopic ratios are 0.15%; and the in-run precision ($2\sigma_m$) is generally better than 0.07%.

tonic setting of volcanic rocks has become increasingly popular. However, due to several factors, such as, imprecise chemical analysis, post-magmatic alteration, and indiscriminant chemical parameters employed, etc., misuse and sometimes abuse of geochemical diagrams have also increased in the literature. The interpretation of ophiolitic complexes has been further complicated by the fact that there are too many overlaps in geochemical and isotopic characteristics between volcanic rocks formed at mid-ocean ridges and immature island arcs, such as the Marianas (Perfit et al. 1980). On the other hand, the long-held view of the Troodos Ophiolite as formed at an oceanic spreading center (Moores and Vine 1971; Gass et al. 1975) was first challenged by Miyashiro (1973) on the basis of the peculiar calc-alkaline nature of the Upper Pillow Lavas. Miyashiro (1973) proposed an island arc origin for these lavas, and this hypothesis was later supported by more elaborate trace element and isotopic data (Schmincke et al. 1983; Robinson et al. 1983; McCulloch and Cameron 1983; Rautenschlein et al. 1985). Most recently, the Troodos Complex has been reinterpreted by Moores et al. (1984) as formed in a tectonic setting where sea floor spreading takes place in short segments above a subduction zone in the region of active spreading. A similar interpretation has also been given to

Table 1. Average compositions of mafic rocks from the East Taiwan Ophiolite (ETO)

	Pillowed Basalts	Dolerites	Gabbros	MORB	Island Arc basalts (IAB)
No. of analysis	(34)	(31)	(22)	(590)	
SiO_2 (%)	49.20 ± 1.21 (σ)	49.23 ± 4.04	50.83 ± 3.29	50.53	51.56
Al_2O_3	15.60 ± 0.96	14.72 ± 2.84	17.99 ± 2.40	15.27	17.51
Fe_2O_3*(or FeO*)	11.03 ± 0.96	9.89 ± 2.93	6.51 ± 1.79	10.46	9.25
MnO	0.15 ± 0.03	0.16 ± 0.06	0.09 ± 0.03	0.16	0.17
MgO	8.93 ± 0.96	9.02 ± 3.93	7.08 ± 1.81	7.47	6.19
CaO	11.05 ± 0.78	10.27 ± 2.36	12.53 ± 2.67	11.49	10.35
Na_2O	2.48 ± 0.32	2.43 ± 0.84	2.40 ± 0.55	2.62	2.65
K_2O	0.17 ± 0.12	0.39 ± 0.22	0.52 ± 0.48	0.16	0.85
TiO_2	0.93 ± 0.21	0.96 ± 0.64	0.73 ± 0.56	1.56	0.89
P_2O_5	0.12 ± 0.05	0.15 ± 0.15	0.11 ± 0.09	0.13	0.19
LOI	1.87 ± 1.33	3.04 ± 1.69	1.75 ± 0.85	–	–
Total	101.55	100.25	100.53		

Sources: ETO: Liou et al. (1977); Juan et al. (1978, 1980); New data (Table A-1, Appendix). MORB: Melson et al. (1976), on ~ 590 analyses of glasses from all spreading centers. Island Arc basalts: Ewart (1976)

Note: Fe_2O_3 as total Fe for ETO; FeO as total Fe for MORB and IAB

Results

Major element data

New major element data are presented in Table A-1 in Appendix 1. A compilation of available chemical analyses including those already published by Liou et al. (1977) and Juan et al. (1978, 1980) reveals that the basalts and the dolerites of the ETO have strikingly similar compositions, whereas the gabbros, as expected, show more variable and differentiated natures (Table 1, Figs. 2, 3, 4).

In an AFM diagram (Fig. 2), the data for pillow basalts and dolerites cluster within a rather restricted field defined by ocean floor tholeiites (Shido et al. 1971). However, the greater scatter of dolerite data implies a more pronounced effect of fractional crystallisation. This is also reflected in a normative plot (Fig. 3) and in the range of their mg values (molecular ratios of $Mg/(Mg + Fe^{++})$, assuming $Fe_2O_3 = 0.1 \times$ total Fe as FeO, Fig. 4). Figure 3 shows a normative basalt composition diagram projected from the plagioclase apex. A few glass samples of the ETO are Q-normative and none are Ne-normative. The distribution of data points for basalts and dolerites is entirely comparable with MORB (Bence et al. 1979), as well as with island arc tholeiites (IAB, Perfit et al. 1980).

The rather limited range of mg values (69 to 57, except for one sample of 78, Fig. 4) for pillow basalts suggests that they have not undergone extensive fractional crystallisation. By contrast, both dolerites and gabbros have greater variation in mg values, ranging from 80 to 55; these rocks evidently are more differentiated than the glassy basalts.

The TiO_2 contents in practically all pillow basalts of the ETO lie within the field of MORB glasses (Fig. 4). Similarly, dolerite data fall within the field of crystalline MORB. On the other hand, substantial amount of IAB data are found to overlap the field of crystalline MORB in the TiO_2 vs mg diagram, even though their areas of distribution are distinguished from those of MORB (Perfit et al. 1980). The TiO_2 contents of glassy basalts of the ETO range from 0.5% to 1.5% with a mean of 0.93% (Table 1), which is not distinguishable from the average value (0.89%) of IAB
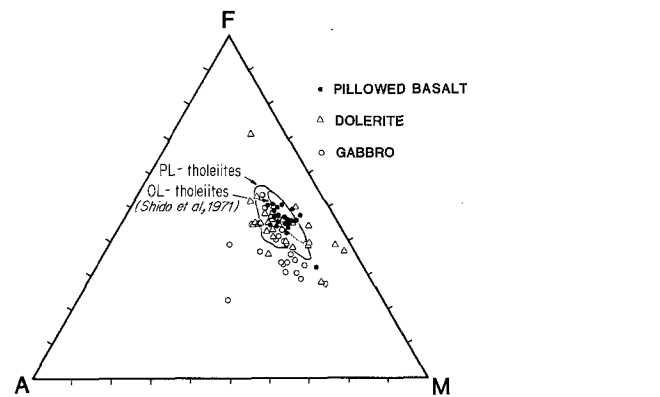

Fig. 2. Compositional ranges of mafic rocks from the ETO. Basalt and dolerite data are generally confined within the envelops of mid-ocean ridge basalts
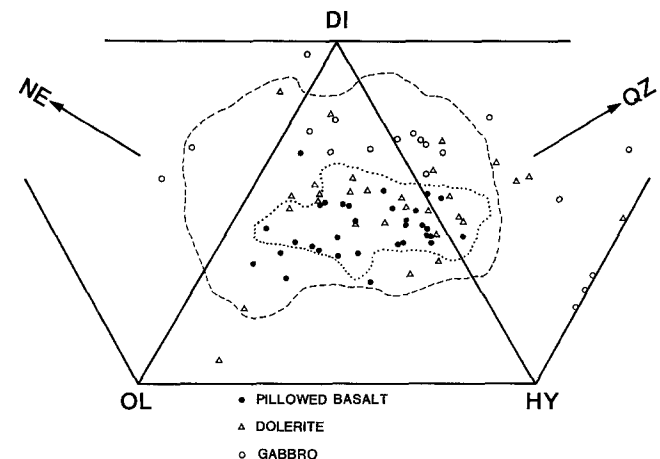

Fig. 3. Normative compositions of mafic rocks from the ETO projected from plagioclase. *Dotted line envelop* = field for the majority of MORB glasses; *dashed line envelop* = field for the majority of crystalline MORB (Bence et al. 1979)
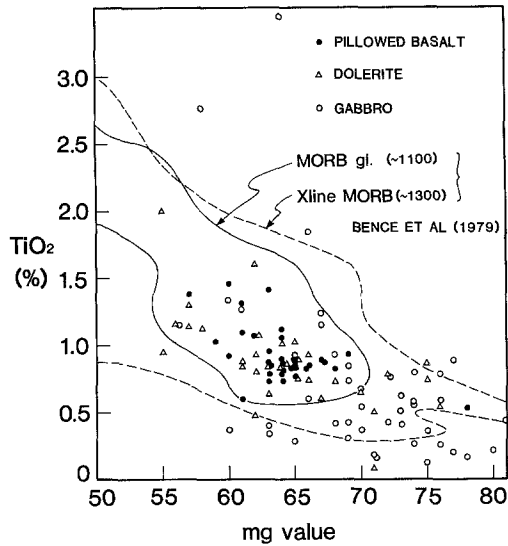
Fig. 4. Diagram of TiO_2 vs mg value for mafic rocks of the ETO. The basalt data are completely compatible with the MORB glass data of Bence et al. (1979), despite of a much smaller variation in TiO_2 contents for ETO rocks

compiled by Ewart (1976). Although the mafic assemblage of the ETO have the major element characteristics typical of MORB, these chemical criteria do not sufficiently prove that they have been formed in a mid-ocean ridge environment, simply because the above chemical variation diagrams (Figs. 2, 3 and 4) have no resolving power in discriminating MORB from IAB.

Rare earth element distribution patterns

REE concentration data are presented in Table 2 and the chondrite-normalised distribution patterns are shown in Figs. 5 through 9. The basaltic glass samples show two distinct types of REE patterns, one with LREE (light REE) enrichment which is equivalent to a P-type MORB pattern, and the other with LREE depletion which is typical of the much more abundant N-type MORB (Fig. 5). The recognition of both P- and N-type basalts in the ETO has never been so clearly demonstrated by previous geochemical studies. Transitional type (T-type) basalts probably also exist despite the fact that they are not shown by the present analyses. The coexistence of both P- and N-type basalts has been found in a genuine ocean ridge environment, such as those from DSDP Hole 504B of the Costa Rica Rift of the East Pacific Rise system (Fig. 6; Tual et al. 1985).

In an earlier study of trace element geochemistry, Chou et al. (1978) showed that most basalts, dolerites and gabbros from the ETO have LREE-depleted patterns. Nevertheless, they have also reported a dolerite (No. 76-023) with LREE-enriched pattern quite similar to those of the P-type basalts shown here in Fig. 5. The LREE-enriched P-type magmas could not have been derived by fractional crystallisation from N-type magmas as deduced from a simple modelling calculation. Consequently, it is inferred that at least two distinct mantle source regions have been involved in the generation of the different types of basaltic magmas. Transitional type basalts may be formed as a result of magmatic mixing.

Fig. 7 shows the depleted nature of REE patterns for three gabbros and a hornblendite. The hornblendite sample
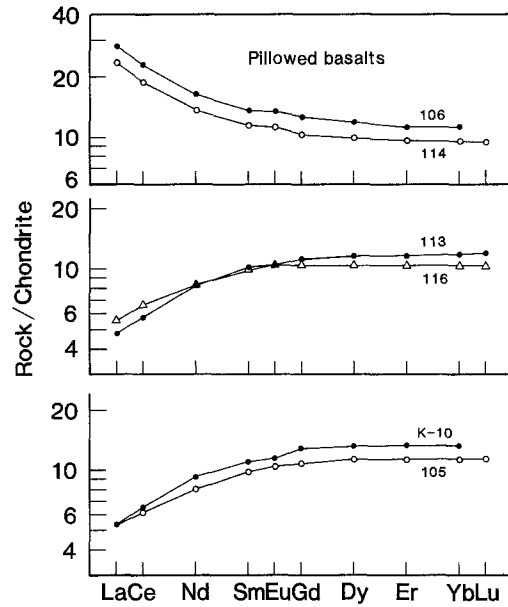

Fig. 5. REE distribution patterns for pillow basalts (glasses) of the ETO. K-10 is from Sun et al. (1979). Samples 106 and 114 are P-type basalts with enriched LREE, the others are N-type basalts with LREE depletion
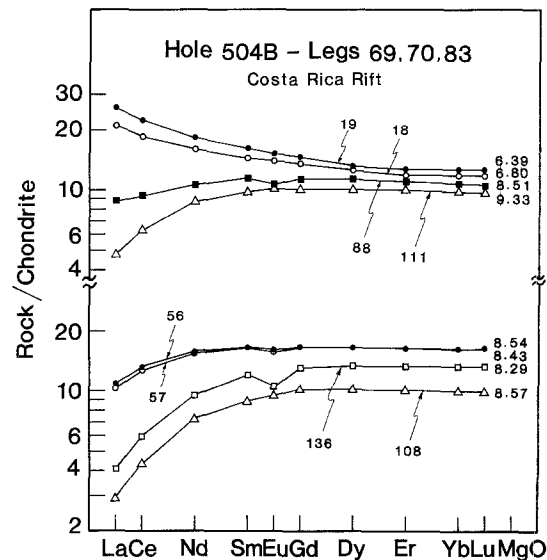

Fig. 6. Coexistence of both N- and P-type basalts in a single site of oceanic crust (Data from Tual et al. 1985). Note the extraordinary resemblance of REE patterns in these oceanic tholeiites and in the ETO basalts

was collected from a highly weathered and physically disintegrated dike which cuts a gabbroic body. The purpose of this analysis was to examine the REE mobility problem in such conditions. The extensive alteration effect has apparently resulted in pronounced loss in mobile elements such as K, Rb, Sr and Ba, but no conclusive effect can be ascerntained for the less mobile elements (Table 2). The extremely low Sr (6 ppm) and Ba (trace) contents have been double-checked, hence are not due to analytical accident. With regard to the REE pattern, the distinct negative Eu anomaly is believed to be the outcome of surface weathering/alteration process and should bear no petrogenetic

Table 2. Trace element abundances of the East Taiwan Ophiolite

Sample no.	102W	103	104	105	106	107	108	110A	110B
Rock type	Rodin. gabbro	harz-burgite	Gabbro	basalt	basalt	hornbl-endite	Serpen-tinite	Plagio-granite	Plagio-granite
All concentrations in ppm									
La	0.44	0.029	0.690	1.680	8.81	1.920	0.031	3.96	3.94
Ce	0.831	0.055	2.150	5.03	18.70	10.26	0.052	7.87	7.81
Nd	0.620	0.021	2.022	4.81	9.82	17.03	0.021	4.93	4.77
Sm	0.198	0.004	0.784	1.897	2.653	7.83	0.0052	1.877	1.81
Eu	0.170	0.0008	0.396	0.761	0.983	1.800	0.0068	0.717	0.684
Gd	0.275	–	1.190	2.860	3.360	11.80	0.0062	2.864	2.68
Dy	0.346	0.0076	1.575	3.745	3.93	15.48	0.0115	4.012	3.85
Er	0.226	0.0084	1.065	2.435	2.422	10.05	0.0135	2.705	2.585
Yb	0.220	0.017	1.053	2.400	2.388	9.87	0.024	2.719	2.580
Lu	0.035	0.0047	0.167	0.376	–	1.525	0.007	0.394	0.370
$(La/Sm)_N$		4.4	0.54	0.54	2.02	0.15	3.6	1.3	1.3
Rb		<1		2.5	10.7	<1	1	1	
Sr		96		89	182	6	tr	94	
Ba		3				tr	2	53	
Zr		3		53	86	48	2	254	
Nb		tr		2	14.9	4	tr	14	
Y		tr		25.1	25.9	107	1	41	
Ti									
Sc									
Ni		2,370		145	132	553	2,255	35	
Co		104		44	46	31	101	4	
Cr				375	262				
V		64		227	221	670	35	11	

Note: (1) Data of K-10 from Sun et al. (1979); (2) Chondrite normalisation values based on the Leedey abundances (Masunda et al., 1973) dividede by 1.2.
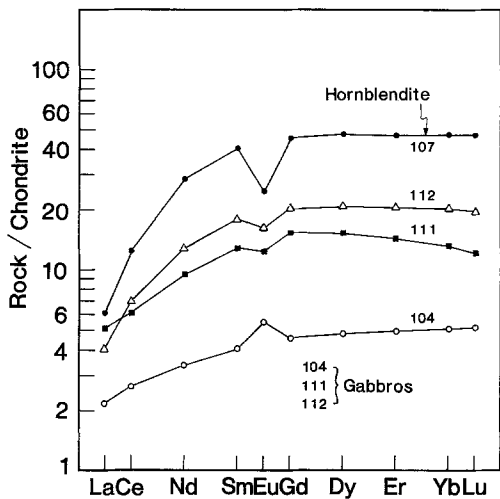

Fig. 7. REE distribution patterns of a hornblendite and three gabbros

Fig. 8. REE distribution patterns of a rodingitized gabbro and two highly serpentinized ultramafic rocks

significance. However, the LREE-depleted nature appears to be genuine and inherited from its source characteristics, even though slight modification of LREE distribution and overall concentration level is considered possible.

The gabbros have both positive- (No. 104) and negative-Eu anomalies (Nos. 111 and 112), probably signifying an important role of plagioclase in fractional crystallisation (Fig. 7). Sample 104 shows a net effect of plagioclase cumulation, whereas the two others might have had plagioclase extraction from their parental magmas. The LREE-de-
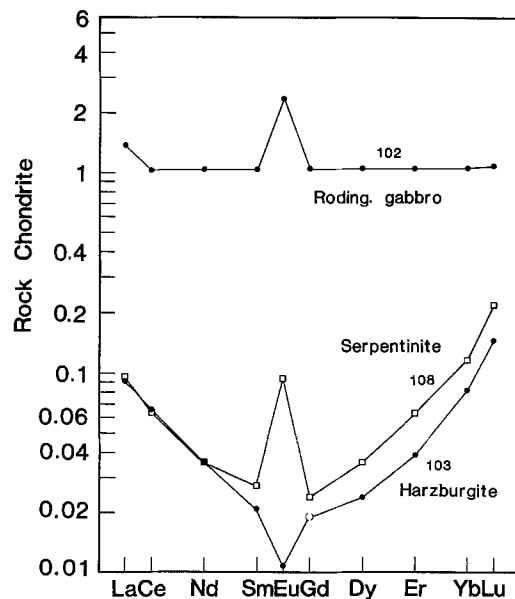
pleted nature as observed in all gabbros once more indicates that their source regions are quite similar to those of the associated N-type basalts (Fig. 5). However, the geological arguments derived from the petrographic characteristics of the inter-sequence red shales favor a model that the plutonic sequence including the gabbros was emplaced long before (perhaps 10 Ma or longer) the deposition of the extrusive sequence about 15 Ma ago (Ernst and Liou 1985).

Sample no.	111	112	113	114	116	117	K-10	Chondrite
Rock type	Gabbro	Gabbro	basalt	basalt	basalt	red shale	basalt (1)	(2)

All concentrations in ppm

	111	112	113	114	116	117	K-10	Chondrite
La	1.622	1.273	1.480	7.35	1.758	31.69	1.70	0.315
Ce	4.98	5.67	4.66	15.35	5.45	64.8	5.43	0.814
Nd	5.66	7.72	4.92	8.26	5.02	27.38	5.53	0.597
Sm	2.490	3.45	1.945	2.229	1.882	5.58	2.14	0.192
Eu	0.899	1.17	0.763	0.823	0.756	1.267	0.850	0.0723
Gd	3.99	5.237	2.916	2.682	2.748	4.98	3.39	0.259
Dy	4.99	6.80	3.855	3.246	3.475	4.52	4.33	0.326
Er	3.05	4.39	2.533	2.070	2.234	2.797	2.89	0.213
Yb	2.73	4.20	2.490	1.996	2.182	2.527	2.78	0.208
Lu	0.392	0.632	0.391	0.309	0.331	0.378	–	0.0323
$(La/Sm)_N$	0.40	0.22	0.46	2.00	0.57	3.5	0.48	
Rb	13		1.1		0.8	182	3.7	
Sr	342		70		109	89	91	
Ba	386					330	16	
Zr	50		47		50	119	44	
Nb	5		0.8		1.4	11	1.0	
Y	43		25.6		21.3	36	26	
Ti							5,200	
Sc							44	
Ni	120		157		207	340	168	
Co	28		44		51	45	–	
Cr			391				434	
V	590		251			126	255	

Rodingitization of gabbroic rocks is found in many localities in the ETO (Liou et al. 1977). As for the hornblendite described above, it is of great geochemical interest to understand REE behavior under extreme alteration/metasomatism conditions. Sample 102 (Fig. 8) shows an essentially flat REE pattern of about 1 × chondritic abundances with a slight La enrichment (also double-checked). If the original rock possessed a pattern similar to those of gabbros as shown in Fig. 7, then rodingitization may have produced the following effects: (1) overall decrease in total REE concentrations; (2) possible but uncertain enrichment in Eu and in LREE relative to HREE, especially for La. The heavy rare earths (HREE) appear to remain unfractionated as found in the hornblendite sample and in several case studies of alteration (Frey et al. 1974; Ludden and Thompson 1978, 1979). Obviously, a single analysis is not sufficient to make a generalisation on the effect of rodingitization.

A serpentinite (No. 108) and a harzburgite (No. 103) show similar U- or V-shape REE patterns (Fig. 8). The distinct positive and negative Eu anomalies are believed to be irrelevant to their magmatic processes; instead, they are more likely to be induced by alteration/serpentinisation. U- or V-shape patterns are commonly observed in harburgites and dunites (alpine peridotites) of orogenic zones and ophiolite complexes (Pallister and Knight 1981; Frey 1984). Their total REE contents range generally from 0.01 to 0.2 × chondritic abundances. Interestingly, such REE patterns (very low abundances and U-, V-shaped) have also been found in some achondrites (ureilites, Wänke et al. 1972; Boynton et al. 1976). Consideration of melting relationships and REE distribution coefficients leads to the conclusion that these patterns could not have been produced by simple magmatic processes; in other words, they do not represent

residues left behind by removal of basaltic magmas during partial melting of either chondritic or LREE-depleted mantle peridotites. Melting of such mantle peridotites and extraction of basaltic magma would normally leave a residue characterised by severe LREE depletion and weak HREE fractionation. The relative enrichment of both LREE and HREE in the U-shape patterns strongly implies the role of secondary process, such as metasomatism during serpentinisation, although the exact cause is not known at present.

Red shale or deep-sea clay has been thought to be derived from decomposed volcanic ejecta and pyroclastics, or by aeolian transport of dust material from continental regions. The chemical compositions of red shales from the ETO are highly variable, especially in SiO_2 contents (37 to 60%, Liou et al. 1977). The REE distribution pattern of the particular sample analysed (No. 117, Fig. 9) has a clear "continental" or "granitic" signature with LREE enrichment and typical negative Eu anomaly. The dominant continental component of the red shale is fully supported by the Nd isotopic data to be shown later.

Plagiogranites of the ETO occur as dike rocks and their chemical compositions are highly variable, with SiO_2 contents ranging from 55 to 76% (Liou et al. 1977). They are all soda-rich ($Na_2O = 6–12\%$) and potash-poor ($K_2O = 0.02–0.3\%$), hence are identified with the rock types of trondhjemite/tonalite. Although similar in major element compositions, oceanic plagiogranites or plagiogranites from ophiolitic complexes are readily distinguished from the Archean trondhjemite/tonalite suite in REE distribution patterns. Archean trondhjemites are characterised by highly fractionated REE patterns with LREE enrichment and concomitant HREE depletion. The degree of fractionation is generally expressed by the chondrite-normalised $(La/Yb)_N$
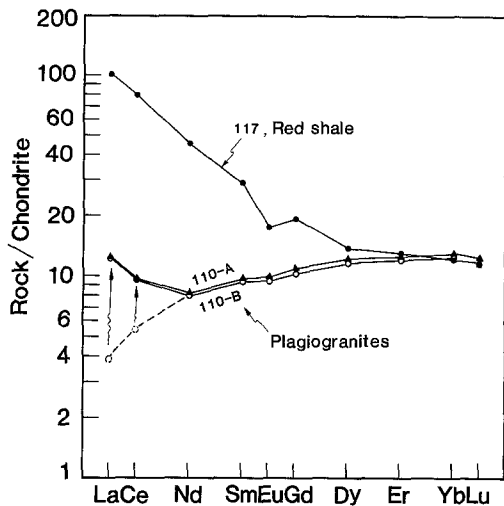
Fig. 9. REE distribution patterns of a red shale and two splits of plagiogranite. The red shale has a typical "granitic" pattern. The plagiogranite might have an original pattern as shown by the dashed trend for La and Ce, which were probably enriched to the present concentration levels during alteration processes

ratio in the rock concerned. Archean rocks usually have $(La/Yb)_N$ ratios between 20 to 40 (40 or greater are not uncommon, see e.g., Jahn et al. 1981), whereas modern oceanic plagiogranites commonly possess ratios less than 1, meaning flat or LREE-depleted patterns. The two REE analyses of plagiogranite splits (see Table A-1 for major element composition) yielded somewhat strange patterns (Fig. 9). Except for La and Ce, the patterns are grossly similar to those of N-type basalts. LREE are generally believed to be more mobile than middle and heavy REE, hence the concentrations of La and Ce in this particular plagiogranite might have been enriched during alteration processes as seen in ultramafic rocks and rodingitized gabbro (Fig. 8). Nevertheless, the general shape of the REE patterns suggests that the plagiogranites were derived from a source depleted in LREE such as that of N-type basalts.

A detailed and lengthy discussion on the petrogenesis of plagiogranites is beyond the scope of this paper and is certainly not justified with only a couple of analyses. The origin of plagiogranites is still controversial; or it may be more correct to state that there are multiple modes of origin for the plagiogranites from ocean floors and from ophiolite complexes. These include (1) hydrous partial melting of oceanic basalt (Helz 1976; Gerlach et al. 1981b), (2) extensive degrees (greater than 80%) of fractional crystallisation from tholeiitic magma (Coleman and Peterman 1975; Stern 1979; Pallister and Knight 1981; Spulber and Rutherford 1983), and (3) immiscibility of highly differentiated silicate liquid (Dixon and Rutherford 1979). It has been demonstrated in hydrous melting experiments (Helz 1976) that the phase assemblage of solid residue is dominated by hornblende and lesser amount of feldspar at lower degrees (<50%) of melting and by hornblende and less pyroxene at higher degrees (>50%). Because the REE K_D values (distribution coefficients) for hornblende in equilibrium with acid liquids are between 4 to 10 for HREE (Hanson 1978), the bulk distribution coefficients (D) for the solid residue would be greater than 2 in any justifiable phase combination. Consequently, if plagiogranite were derived by partial melting of oceanic basalt (HREE = 12 × chon.),

the acid liquid would have much reduced HREE to about 5× chondritic abundances or less. This is not consistent with the observed REE pattern (Fig. 9). Thus the plagiogranite of the ETO is unlikely to be produced by a partial melting process. Although the origin of plagiogranite through fractional crystallisation was favored by field and petrographic observations (Liou et al. 1977), it is rather difficult to reconcile with the low REE abundances for this particular sample (Fig. 9). More analyses on other plagiogranites are needed to further test this model.

The immiscibility hypothesis predicts the coexistence of plagiogranite with Fe-enriched basalt (Dixon and Rutherford 1979), but such Fe-enriched basalt has not been found in the ETO. More recently, Spulber and Rutherford (1983) showed in an hydrothermal experiment that plagiogranite could be derived from basaltic magma by extensive fractional crystallisation.

REE are generally immobile in alteration/metamorphism conditions. However, in some cases of highly altered (e.g., hornblendite, Fig. 7) and serpentinized (e.g., rodingite, harzburgite, Fig. 8) rocks, and particularly of those ultrabasic rocks containing low REE abundances, the REE patterns could be modified to some extent, especially in terms of their LREE distributions. It must be also acknowledged that there is no simple relation between the degree of REE mobility and the intensity of alteration, the grade of metamorphism and the type of rock being altered (see review by Humphris 1984). Moreover, the enrichment or depletion of more mobile LREE relative to HREE is generally not predictable, nor is the occurrence of Eu anomalies.

Despite the above problems, it is concluded that the REE patterns obtained from the basaltic glass samples, the gabbros and the red shale (Figs. 5, 7, and 9) have not been appreciably modified and they may be used in petrogenetic discussion. Except for La and Ce, the overall REE distribution pattern of plagiogranite (Fig. 9) appears to argue for a close genetic link with the N-type basalts of the ETO.

Isotope geochemistry

(1) Nd isotopic compositions. Sm-Nd isotopic data for some selected samples are presented in Table 3. Except for the red shale sample (No. 117, prefix BJ and postfix 82 omitted hereafter), all $^{143}Nd/^{144}Nd$ ratios are higher than that of the bulk earth (BE) or the chondritic value (CHUR) of 0.51264. In other words, they all have positive ε_{Nd} values, even for the P-type basalt (No. 106). The range of ε_{Nd} values suggests that, as common to most modern oceanic basalts, their source regions have been non-uniformly depleted in LREE relative to CHUR over a long period of time (≥ 1 Ga) as evidenced from the calculated model ages T_m (Table 3). The constraint of REE distribution requires a derivation of P-type basalt from a mantle peridotite enriched in LREE, but the isotopic data ($\varepsilon_{Nd} = +8.7$) suggests the enrichment to be a rather recent phenomenon.

Recent MORB have a small range of ε_{Nd} values, with a mean of about +10 (DePaolo and Wasserburg 1976; O'Nions et al. 1977). Island arc volcanic rocks commonly have positive ε_{Nd} values that substantially overlap with those of MORB. However, White and Patchett (1984) have recently demonstrated on a statistical basis that the highest ε_{Nd} values of MORB ($\geq +12$) have not been found in island arc volcanics, and they are the unique and most diagnostic characteristics of typical N-type MORB. The few high ε_{Nd}

Table 3. Sm-Nd Isotopic data of the East Taiwan Ophiolite

Sample no.	Rock type	$^{147}Sm/^{144}Nd$	$^{143}Nd/^{144}Nd \pm 2\sigma_m$		$\varepsilon_{Nd}(0)$	T_m (Ga)
BJ-106-82	basalt (P)	0.164	0.513085	22	+8.7	−2.12
BJ-107-82	hornblendite	0.280	0.513235	24	+11.6	1.09
BJ-110-82	plagiogranite	0.232	0.513300	25	+12.9	2.86
BJ-111-82	peg. gabbro	0.268	0.513310	34	+13.1	1.43
BJ-113-82	basalt (N)	0.240	0.513320	24	+13.3	2.35
BJ-116-82	basalt (N)[a]	0.228	0.513127	17	+9.5	2.36
BJ-117-82	red shale	0.124	0.512323	25	−6.2	0.666

[a] Nd isotopic composition of this sample was determined using the mass spectrometer Minmass 1 of the University of Minnesota in June 1984

Note: $^{147}Sm/^{144}Nd$ (CHUR) = 0.1967; $^{143}Nd/^{144}Nd$ (CHUR,0) = 0.51264

Definitions:

$$\varepsilon_{Nd}(0) = \left[\frac{(^{143}Nd/^{144}Nd)m}{0.51264} - 1 \right] \times 10^4$$

$$T_m = \frac{1}{\lambda} \ln \left[1 + \frac{(^{143}Nd/^{144}Nd)m - 0.51264}{(^{147}Sm/^{144}Nd)m - 0.1967} \right], \quad \text{where, } \lambda = 0.00654 \text{ Ga}^{-1}.$$

All measured $^{143}Nd/^{144}Nd$ ratios have been normalized against the value of 0.7219 for $^{146}Nd/^{144}Nd$.

values ($\geq +12$) measured in basalts of the ETO (Table 3) are probably the best evidence for its origin at a mid-ocean ridge environment.

The Troodos Ophiolite has long been considered as a model of obducted oceanic crust (Moores and Vine 1971; Gass et al. 1975). Recently, petrological and geochemical arguments have strongly changed the orthodox view of mid-ocean origin of the ophiolite to the formation in an island arc environment, or in a back-arc spreading center above a subduction zone (Miyashiro 1973; Pearce 1982; Schmincke et al. 1983; Robinson et al. 1983; Moores et al. 1984; Rautenschlein et al. 1985). At any rate, the common presence of calc-alkaline nature in island arc magmas is implied, and the usual influence of continental materials or sediments in magma genesis is clearly reflected by the observed variable and lower ε_{Nd} values ($+7.9$ to $+0.8$, McCulloch and Cameron 1983). The case for the Troodos Ophiolite is certainly different from that for the East Taiwan Ophiolite.

The Nd isotopic compositions of hornblendite and gabbro (Table 3) are similar to those of the N-type basalts, suggesting that the intrusive rocks and the basalts have a common source with LREE-depleted characteristics. On the other hand, the negative ε_{Nd} value (-6.2, Table 3) found for the red shale sample clearly indicates the dominance of continental REE components in its derivation. The Nd isotopic composition is also entirely comparable with that of Pacific pelagic clays, which are generally more radiogenic than those of the Atlantic and Indian oceans (Piepgras et al. 1979; Goldstein and O'Nions 1981). On the basis of REE distribution pattern and Nd isotopic composition, the red shales from the ETO have all the characteristics of modern pelagic clays from the Pacific ocean, and it was mainly derived by weathering of continental material (granitoids), probably from the eastern Asiatic continent.

(2) Sr isotopic compositions. Sr isotopic data have been reported by Chou et al. (1978) for various rock types from the ETO. $^{87}Sr/^{86}Sr$ ratios of 4 glassy basalts range from 0.7041 to 0.7048; of 4 gabbros from 0.7033 to 0.7036; and of 3 dolerites (5 measurements) from 0.7036 to 0.7072. A

new measurement on pegmatitic gabbro (BJ-111-82) gave 0.70604 ± 5. In all cases, the Sr isotopic ratios are greater than the entire range of fresh MORB (0.7022–0.7033, mean = 0.7027, Hofmann and Hart 1978), but the observed values are not unusual for ocean floor basalts that have undergone sea water alteration and Sr isotope exchange (Hart 1971; Hart et al. 1974; Jahn et al. 1980b; Staudigel et al. 1981). Sr isotope exchange is not necessarily accompanied by visible Nd isotope exchange because Nd is much more resistant to alteration than Sr, and the concentration of Nd is much lower (about 10^{-6}) than that of Sr in sea water. Consequently, the use of Sr isotopic ratios in assessing tectonic environment is suspect. Nevertheless, the possibility that the relatively high Sr isotopic ratios result from a contribution of recycled crustal materials or altered oceanic crust during magmagenesis is not entirely ruled out here, but this possibility remains remote in view of the Nd and Pb isotopic arguments below. Although the reported $^{87}Sr/^{86}Sr$ ratios for the ETO (0.7033 to 0.7047, except for one case of 0.7072, Chou et al. 1978) are within the range of those for island arc volcanic rocks (Whitford 1975; Hawkesworth 1982; White and Patchett 1984), the present Nd isotopic compositions and REE patterns do not favor an island arc interpretation as given by Chou et al. (1978). Sr analyses of the Samail Ophiolite of Oman, believed by some to be the best candidate for obducted oceanic crust to date (Coleman 1981), also indicate an important variation in initial $^{87}Sr/^{86}Sr$ ratios as a result of hydrothermal exchange (McCulloch et al. 1980; Lanphere et al. 1981). Pearce et al. (1981), however, considered that the Samail Ophiolite to be a fragment of a submarine arc-basin complex formed above a subduction zone.

(3) Pb isotopic compositions. Pb isotopic compositions of the ETO rocks have been reported by Chou et al. (1978) and Sun (1980). These values and the new data are presented in Table 4. All isotopic ratios have been adjusted to a set of common Pb standard values and are now directly comparable. The isotopic data are shown in Fig. 10, together with some reference fields for MORB of the Pacific, Samail Ophiolite, andesites of Taiwan and Pacific oceanic

Table 4. Pb isotopic compositions of the East Taiwan Ophiolite

Sample no.	Rock type	$\dfrac{^{206}Pb}{^{204}Pb}$	$\dfrac{^{207}Pb}{^{204}Pb}$	$\dfrac{^{208}Pb}{^{204}Pb}$
BJ-105-82	basalt glass (N)	17.884	15.398	37.578
BJ-106-82	basalt glass (P)	18.216	15.467	38.127
BJ-113-82	basalt glass (N)	17.810	15.470	37.720
BJ-114-82	basalt glass (P)	18.274	15.493	38.243
BJ-116-82	basalt glass (N)	17.936	15.493	37.766
K 315 (1)	basalt glass	18.506	15.485	38.323
TK 403 (1)	basalt glass	18.573	15.528	38.536
T 504a (1)	basalt glass	17.895	15.377	37.611
T 504b (1)	basalt glass	17.892	15.365	37.579
T 507 (1)	basalt glass	17.921	15.393	37.658
K 11 Alb (2)	pillowed basalt	18.015	15.468	37.727
TPY 6458 (2)	pillowed basalt	18.005	15.450	37.788
76-010 (1)	dolerite	18.047	15.479	37.774
76-017a (1)	dolerite	17.857	15.392	37.731
76-023a (1)	dolerite	18.479	15.435	38.280
76-023b (1)	dolerite	18.488	15.450	38.308
BJ-104-82	gabbro	17.950	15.530	39.493
BJ-111-82	peg. gabbro	17.835	15.420	37.732
BJ-112-82	gabbro	17.562	15.443	37.453
76-003 (1)	gabbro	17.973	15.406	37.739
76-004 (1)	gabbro	17.876	15.381	37.526
76-006 (1)	gabbro	17.960	15.420	37.662
76-007 (1)	gabbro	17.848	15.456	37.601
K8 A 1 a (2)	gabbro	17.952	15.457	37.781
K10 A 2 b (2)	gabbro	18.060	15.461	37.698
76-027 (1)	peridotite	18.519	15.653	39.078
76-028 (1)	peridotite	18.553	15.560	38.128
BJ-110-82	plagiogranite	17.920	15.438	38.450
NBS-981	(certified value)	16.937	15.491	36.721

Note: All values have been adjusted to the certified values of Catanzaro et al. (1968). Data sources: (1): Chou et al. (1978), (2): Sun (1980)

Fig. 10. Pb isotopic compositions for various rock types of the ETO. Data sources used for reference fields: Tatsumoto (1978), Sun (1980), Chen and Pallister (1981), Cohen and O'Nions (1982), Hamelin et al. (1984a), White (1985). Penghu alkali basalts are from the Penghu Archipelago, Taiwan Strait; Samail = Samail Ophiolite of Oman

sediments. As pointed out by Chou et al. (1978), the rocks of the ETO may be divided into two groups according to their Pb isotopic compositions: Group 1 consists of rocks with lower $^{206}Pb/^{204}Pb$ ratios (17.8–18.1) and Group 2 with higher ratios of about 18.5 (Fig. 10). However, with the addition of new data, this two-fold grouping becomes less clear and it appears that the field for the ETO is enlarged and intermediate compositions also exist. Nevertheless, the majority of isotopic data for basalts and gabbros are more or less confined within the field defined for MORB of the Pacific Ocean (Tatsumoto 1978; Sun 1980; Hamelin et al. 1984). They are practically identical to those of the Samail Ophiolite (Chen and Pallister 1981).

Some basalts and dolerites of the ETO are more radiogenic, suggesting that they might have been derived from a different source from less radiogenic rocks. As mentioned earlier, the P-type basalt (No. 106) has a less radiogenic Nd isotopic composition, hence its source could have been enriched in LREE in relatively recent time, perhaps less than 500 Ma, depending on melting models. It is likely that such an enrichment event have also enriched the U/Pb and Th/Pb ratios, thus made the source region to experience a more rapid radiogenic growth in Pb isotopic ratios. The new data indeed show an excellent internal consistency with
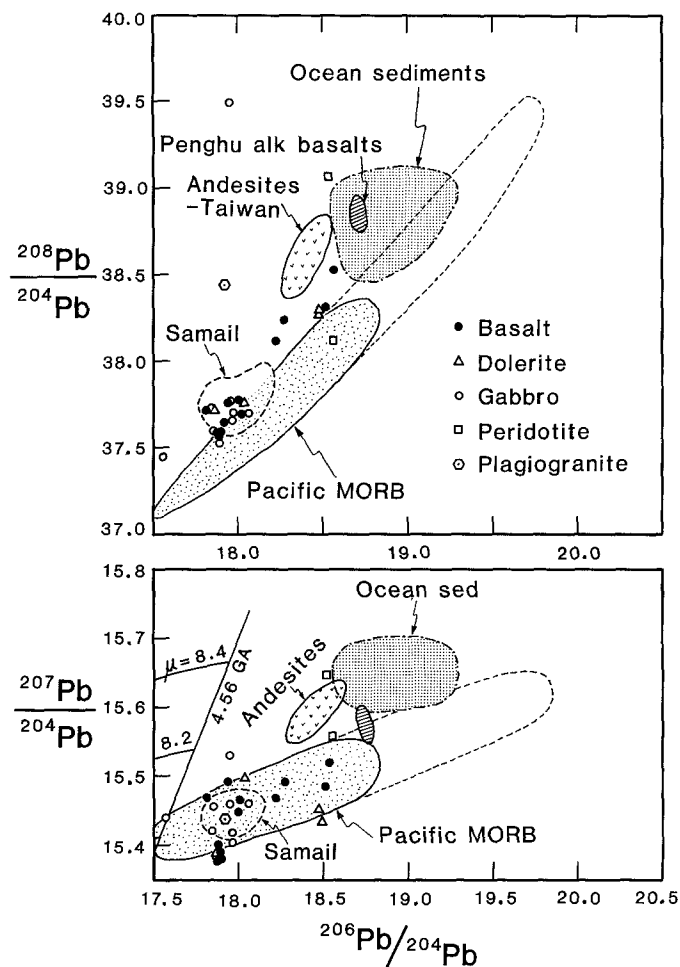
this prediction. The P-type basalts (Nos. 106 and 114) have higher $^{206}Pb/^{204}Pb$ and $^{208}Pb/^{204}Pb$ ratios than the N-type basalts (Nos. 105, 113 and 116). Moreover, the P-type dolerite (No. 76-023) reported by Chou et al. (1978) also shows an identical relation. The Pb isotopic data, however, do not unequivocally suggest that the enrichment event took place recently.

The $^{207}Pb/^{204}Pb$ and $^{208}Pb/^{204}Pb$ ratios of two serpentinized peridotites (Table 4) are considerably higher than all other mafic rocks (Fig. 10). Because of their very low Pb concentrations (≤ 0.1 ppm, often < 20 ppb, Chen and Pallister 1981; Hamelin et al. 1984b), and the alteration effect already demonstrated by their U- or V-shape REE patterns, it is probable that their isotopic compositions have been modified during the process of serpentinization/alteration. The same interpretation was also favored by Chou et al. (1978). On the other hand, the conspicuous enrichment in $^{208}Pb/^{204}Pb$ for a gabbro (No. 104) and a plagiogranite (No. 111) is not well understood.

It is generally agreed that contribution of continental and sedimentary materials in the generation of island arc magmas is visible and significant. This contribution has been demonstrated by previous Sr, Nd and Pb isotopic studies (Tatsumoto 1969; Armstrong 1971; Meijer 1976; De

Paolo and Wasserburg 1977; Kay et al. 1978; Sun 1980; Hawkesworth and Powell 1980; McCulloch and Perfit 1981; Hawkesworth 1982; Cohen and O'Nions 1982; White and Patchett 1984; Hamelin et al. 1984b). By and large, the Pb isotopic data of the ETO, especially those obtained from fresh basaltic glasses, are consistent with an hypothesis of mid-ocean or marginal basin origin. As shown in Fig. 10, the Pb isotopic compositions of typical island arc volcanic rocks as represented by the andesites of Taiwan are distinctly more radiogenic in terms of $^{207}Pb/^{204}Pb$ and $^{208}Pb/^{204}Pb$ ratios, implying a role of oceanic sediments in their magma genesis.

Conclusions of geochemical characterisation and tectonic implications

The new geochemical and isotopic data presented herein and the available data from the literature indicate that the volcanic and plutonic rocks of the East Taiwan Ophiolite have all the characteristics typical of rocks formed at spreading ridges of open oceans or marginal basins. Although the geochemical data have much in common with those of immature island arc tholeiites, the overall geochemical characteristics (Table 5), particularly the REE distribution patterns, the Pb isotopic compositions and the very high and limited range of positive ε_{Nd} values observed in glassy basalts, gabbros and plagiogranite, suggest that an island arc interpretation is vulnerable. The association of characteristic Pacific-type deep-sea clay with the igneous rocks further attests to a typical ocean floor signature of the ETO.

This conclusion is consistent with that reached by Liou et al. (1977), Liou and Ernst (1979) and Ernst and Liou (1985) from their studies of metamorphic history of the ETO. As summarized by Ernst and Liou (1985), most ophiolitic complexes of the world are pre-Cenozoic in age, and are penetratively deformed and commonly exhibit pervasive effects of continental margin or island arc metamorphism superimposed on phase assemblages formed during an earlier oceanic recrystallisation. The Miocene ETO lacks such mineralogic overprinting, hence the metamorphism (greenschist and zeolite facies) can be assigned unambiguously to processes operating at a spreading center and/or near the surface of the sea floor.

The association of both N-type and P-type basalts in the ETO requires distinct sources for their magma generation. Trace element model calculations suggest that P-type magmas could not have been derived by fractional crystallisation from N-type parental liquids, or vice versa. Because the P-type basalts have a positive ε_{Nd} value, their source regions must have had a time-integrated LREE-depleted nature. The enrichment of LREE in the depleted source could have occurred recently (as recent as 300 Ma), but precise timing cannot be constrained as the origin of P-type source is still controversial.

With regard to the size of ocean in which the ETO was generated, it was probably not a large ocean mainly because of its young age of formation (about 15 Ma, see Appendix 2). The collision of the Luzon Arc with the Asiatic continental margin took place about 4–5 Ma B.P. (Chi et al. 1981). Consequently, the ETO was probably transported to the present site, by erosional processes according to the model of Page and Suppe (1981), sometime earlier

Table 5. Summary of geochemical compatibility of the ETO with diverse tectonic settings (+ + + most compatible, + +compatible, + slightly compatible, −not compatible)

	Mid-ocean ridge (large ocean and marginal basin)	Island Arc	Ocean Island
AFM variation in basalts	+ + +	+ +	+
Di-Ol-Hy variation	+ + +	+ +	+ +
Mg values of basalts and dolerites	+ + +	+ +	+
TiO₂-mg (or MgO) variation in basalts	+ + +	+ +	−
REE distribution patterns	+ + +	+ +	−
Nd isotopic ratios	+ + +	+	−
Sr isotopic ratios	+ + (altered basalts)	+ +	+ +
Pb isotopic ratios	+ + +	+	+ +
Presence and nature of red shale	+ + +	+	−

than 5 Ma B.P. In other words, a life span of no more than 10 Ma is estimated for the ETO between its birth at a spreading axis, its transportation and its death through erosion and final emplacement. If the approaching rate of the Luzon Arc towards the Eurasian plate were taken to be 10 cm/yr, the ETO had then traveled a maximum distance of 1000 km. This would suggest a marginal basin such as the South China Sea as postulated by Suppe et al. (1981). Of course, a large open ocean cannot be entirely ruled out because some segments of present East Pacific Rise are also quite close to the North America continent.

In conclusion, the overall geochemical and isotopic characteristics strongly favor a mid-ocean ridge or marginal basin origin of the East Taiwan Ophiolite, which is probably the most "oceanic" and the "youngest" among the known ophiolite complexes of the world.

Appendix 1. Table A-1: Major element compositions of the East Taiwan Ophiolite

Sample no.	105	106	113	107	111	103	108	110	117	K-10
Rock type	basalt glass	basalt glass	basalt glass	hornbl-endite	gabbro	harz-burgite	fine-gr serpent.	plagio-granite	red shale	basalt
SiO_2(%)	49.52	48.62	49.82	49.58	49.55	38.10	37.11	66.24	51.78	49.96
Al_2O_3	15.24	16.56	15.35	5.07	19.00	0.34	0.33	18.27	17.37	15.32
Fe_2O_3	10.49	11.14	10.02	14.80	6.60	8.53	8.61	0.52	9.02	10.16
MnO	0.16	0.16	0.17	0.18	0.11	0.12	0.13	0.01	0.26	0.17
MgO	8.51	7.65	9.33	15.53	5.85	39.70	39.15	1.16	6.81	9.37
CaO	11.03	10.71	12.05	11.68	8.08	1.11	–	1.23	1.54	11.44
Na_2O	1.80	2.42	2.00	0.69	5.05	0.06	0.09	10.59	1.82	2.09
K_2O	0.08	0.38	0.03	–	0.68	–	–	–	3.41	0.10
TiO_2	0.88	1.10	0.82	0.99	1.84	0.01	0.01	0.31	0.69	0.89
P_2O_5	0.12	0.20	0.10	0.01	0.04	–	–	–	0.11	0.07
LOI	0.99	0.17	0.30	0.67	1.55	12.17	12.51	0.51	5.65	0.83
Total	98.82	99.11	99.99	99.20	98.35	100.14	97.94	98.84	98.46	99.57
mg	64	61	68	70	66	91	91	–	–	67

Note: Data of K-10 from Sun et al. (1979)

Table A-2. K–Ar Age data for the East Taiwan Ophiolite

Sample no.	Rock type	K(%)	$^{40}Ar^*$ (ppb)	Ar atm %	T (Ma)
BJ-110-82	Plagiogranite (WR)	0.041	0.097	94.1	33 ± 5
BJ-111-82	Pegma. gabbro (Hb)	0.118	0.092	97.6	11 ± 4
BJ-114-82	Basalt:				
	(a) glass	0.343	0.356	63.1	14.6 ± 0.4
	(b) xline inter.	0.255	0.146	91.5	8.1 ± 0.9

$\lambda_\beta = 4.962 \times 10^{-10}$ an^{-1}; $\lambda_e = 0.581 \times 10^{-10}$ an^{-1}

Appendix 2. Geochronological information

I. Paleontological data

The red shales of the ETO occur either as cementing matrix of the plutonic breccias or as thin layered sediment capping the breccias (Liou et al. 1977). Petrographically, it consists mainly of silt and clay minerals, probably of continental derivation through aeolian transport (see discussion on REE distribution and Nd isotopes). It generally lacks carbonate constituents but contains a minor pelagic organic component of radiolaria plus sponge spicules (Huang et al. (1979). The red shale was believed to be deposited below the carbonate compensation depth (about 4 km) due to the general absence of carbonate component. However, through their careful research, Huang et al. (1979) have found calcareous nannofossils in 6 out of 72 red shale samples of the ETO. All the fossil-bearing samples were collected from shales occurring as cementing matrix of the plutonic breccias and lying stratigraphically below a layered red shale which is, in turn, overlain by pillow lavas. The nannofossils show various states of preservation as a result of carbonate dissolution below the carbonate compensation depth. Nevertheless, they were identified to belong to the Miocene *Sphenolithus heteromorphus* Zone (NN5) corresponding to an age bracket of 13–15 Ma in the tropical Pacific areas (Huang et al. 1979).

II. K–Ar Data

The K–Ar data (Table A-2) were determined by J.-M. Cantagrel (LA 10-CNRS et Université de Clermont-Ferrand II). No concor-

dant ages were obtained but the Miocene assignment of the ETO formation is generally confirmed. Due to the open system behavior of the K–Ar system, no precise significance is attached to the isotopic dates reported herein.

References

Armstrong RL (1971) Isotopic and chemical constraints on models of magma genesis in volcanic arcs. Earth Planet Sci Lett 12:137–142

Bence AE, Baylis DM, Bender JF, Grove TL (1979) Controls on the major and minor element chemistry of mid-ocean ridge basalts and glasses. In: Talwani M, Harrison CG, Hayes DE (eds) Deep Drilling Results in the Atlantic Ocean: Ocean Crust. Am Geophys Union Washington DC pp 331–341

Boynton WV, Starzyk PM, Schmidt RA (1976) Chemical evidence for the genesis of the ureilites, the achondrite Chassigny and the nakhlites. Geochim Cosmochim Acta 40:1439–1447

Catanzaro EJ, Murphy TJ, Shields WR, Garner EL (1968) Absolute isotopic abundance ratios of common, equal-atom and radiogenic lead isotope standards, J. Res Natl Bur Std A Phys Chem 72A:261–267

Chen, JH, Pallister JS (1981) Lead isotopic studies of the Samail Ophiolite, Oman. J. Geophys Res 86:2699–2708

Chi WR, Namson J, Suppe J (1981) Stratigraphic record of the plate interactions in Coastal Range, eastern Taiwan, Mem Geol Soc China, No. 4:155–194

Chou CL, Lo HJ, Chen JH, Juan VC (1978) Rare earth element and isotopic geochemistry of Kuanshan igneous complex, Taiwan, Proc Geol Soc China, No. 21:13–24

Cohen RS, O'Nions RK (1982) Identification of recycled continental material in the mantle from Sr, Nd and Pb isotope investigations. Earth Planet Sci Lett 61:73–84

Coleman RG (1977) Ophiolites: ancient oceanic lithosphere? Springer Berlin Heidelberg New York

Coleman RG (1981) Tectonic setting for ophiolite obduction in Oman, J Geophys Res 86:2497–2508

Coleman RG (1984) The diversity of ophiolites. Geol Mijnbouw 63:141–150

Coleman RG, Peterman ZE (1975) Oceanic plagiogranite, J Geophys Res 80:1099–1108

DePaolo DJ, Wasserburg GJ (1976) Nd isotopic variations and petrogenetic models. Geophys Res Lett 3:249–252

DePaolo DJ, Wasserburg GJ (1977) The sources of island arcs as indicated by Nd and Sr isotope studies. Geophys Res Lett 4:465–468

Dixon S, Rutherford MJ (1979) Plagiogranites as late-stage immiscible liquids in ophiolite and mid-ocean ridge suites: an experimental study. Earth Planet Sci Lett 45:45–60

Ernst WG, Liou JG (1985) Summary of oceanic metamorphism and inferred tectonic history of the East Taiwan Ophiolite. Ofioliti (in press)

Ewart A (1976) Mineralogy and chemistry of modern orogenic lavas – some statistics and implications. Earth Planet Sci Lett 31:417–432

Frey FA (1984) Rare earth element abundances in upper mantle rocks. In: Henderson P (ed) Rare Earth Element Geochemistry. Elsevier, Amsterdam, 153–203

Frey FA, Bryan WB, Thompson G (1974) Atlantic ocean floor: geochemistry and petrology of basalts from Legs 2 and 3 of the Deep Sea Drilling Project. J Geophys Res 79:5507–5527

Gass IG, Neary CR, Plant J, Robertson AHF, Simonian KO, Smewing JD, Spooner ETC, Wilson RAM (1975) Comments on "The Troodos ophiolite complex was probably formed in an island arc" by A. Miyashiro and subsequent correspondence by A. Hynes and A. Miyashiro. Earth Planet Sci Lett 25:236–238

Gerlach DC, Avé Lallemant HG, Leeman WP (1981a) An island arc origin for the Canyon Mountain ophiolite complex, eastern Oregon, USA Earth Planet Sci Lett 53:255–265

Gerlach DC, Leeman WP, Avé Lallemant HG (1981b) Petrology and geochemistry of plagiogranite in the Canyon Mountain Ophiolite, Oregon. Contrib Mineral Petrol 77:82–92

Goldstein SL, O'Nions RK (1981) Nd and Sr isotopic relationships in pelagic clays and ferromanganese deposits. Nature 291:324–327

Hamelin B, Dupré B, Allègre CJ (1984a) Lead-strontium isotopic variations along the East Pacific Rise and the Mid-Atlantic ridge: a comparative study. Earth Planet Sci Lett 67:340–350

Hamelin B, Dupré B, Allègre CJ (1984b) The lead isotope systematics of ophiolite complexes. Earth Planet Sci Lett 67:351–366

Hanson GN (1978) The application of trace elements to the petrogenesis of igneous rocks of granitic composition. Earth Planet Sci Lett, 38:26–43

Hawkesworth CJ (1982) Isotope characteristics of magmas erupted along destructive plate margins. In: Thorpe RS (ed) Andesites. Wiley, Chichester, pp 549–570

Hawkins Jr Jr (1980) Petrology of back-arc basins and island arcs: their possible role in the origin of ophiolites. In: Panayiotou (ed) Ophiolites. Geol Surv Dept Nicosia, Cyprus, pp 244–254

Hart SR (1971) K, Rb, Cs, Sr and Ba contents and Sr isotope ratios of ocean floor basalts, Philos Trans R Soc Lond, A268:573–587

Hart SR, Erlank AJ, Kable EJD (1974) Sea floor alteration: some chemical and Sr isotopic effects. Contrib Mineral Petrol 44:219–230

Helz RT (1976) Phase relations of basalts in their melting ranges at $P_{H_2O} = 5$ Kb. Part II. melt compositions. J Petrol 17:139–193

Ho CS (1975) An istroduction to the geology of Taiwan: explanatory text of the geologic map of Taiwan. Ministry of Economic Affairs, Republic of China, Taipei

Ho CS (1982) Tectonic evolution of Taiwan: explanatory text of the tectonic map of Taiwan. Ministry of Economic Affairs, Republic of China, Tairpei

Hofmann AW, Hart SR (1978) An assessment of local and regional isotopic equilibrium in the mantle. Earth Planet Sci Lett 38:44–62

Hsu TL (1956) Geology of the Coastal Range, eastern Taiwan. Bull Geol Survey Taiwan, No. 8:39–63

Hsu TL (1976) The Lichi melange in the Coastal Range framework. Bull Geol Survey Taiwan No. 25:87–96

Huang TC, Chen MP, Chi WR (1979) Calcareous nannofossils from the red shale of the ophiolite-melange complex, eastern Taiwan. Mem Geol Soc China No. 3:131–138

Humphris SE (1984) The mobility of the rare earth elements in the crust. In: Henderson P (ed) Rare Earth Element Geochemistry. Elsevier, Amsterdam, pp 153–203

Jahn BM, Auvray B, Blais S, Capdevila R, Cornichet J, Vidal F, Hameurt J (1980a) Trace element geochemistry and petrogenesis of Finnish greenstone belts. J Petrol 21:201–244

Jahn BM, Bernard-Griffiths J, Charlot R, Cornichet J, Vidal F (1980b) Nd and Sr isotopic compositions and REE abundances of Cretaceous MORB (Holes 417D and 418A, Legs 51, 52 and 53). Earth Planet Sci Lett 48:171–184

Jahn BM, Glikson AY, Peucat JJ, Hickman AH (1981) REE geochemistry and isotopic data of Archean silicic volcanics and granitoids from the Pilbara Block, Western Australia: implications for the early crustal evolution. Geochim Cosmochim Acta 45:1633–1652

Juan VC (1964) East Taiwanian petrographic province. Proc Geol Soc China No 7:3–20

Juan VC (1975) Tectonic evolution of Taiwan. Tectonophysics 26:197–212

Juan VC, Lo HJ, Chen CH (1978) Petrochemistry and origin of taiwanite and dolerite, east Taiwan. In: Study and Essays in Commemoration of the Golden Jubilee of Academia Sinica, Taipei, pp 71–102

Juan VC, Lo HJ, Chen CH (1980) Genetic relationships and the emplacement of the exotic basic rocks enclosed in the Lichi mélange, east Coastal Range, Taiwan. Proc Geol Soc China, No. 23:56–68

Kay RW, Sun SS, Lee-Hu CN (1978) Pb and Sr isotopes in volcanic rocks from the Aleutian Islands and Probilof Islands, Alaska. Geochim Cosmochim Acta 42:263–273

Lanphere MA, Coleman RG, Hopson CA (1981) Sr isotopic tracer study of the Samail Ophiolite, Oman. J Geophys Res 86:2709–2720

Liou JG, Lan CY, Suppe J, Ernst WG (1977) The East Taiwan Ophiolite: its occurrence, petrology, metamorphism and tectonic setting. Mining Research and Service Organisation Special Report, No 1, 212 p, Taipei

Liou JG, Ernst WG (1979) Oceanic ridge metamorphism of the East Taiwan Ophiolite. Contrib Mineral Petrol 68:335–348

Ludden JN, Thompson G (1978) Behavior of rare earth element during submarine weathering of tholeiitic basalts. Nature 274:147–149

Ludden JN, Thompson G (1979) An evaluation of the behavior of the rare earth elements during weathering of sea floor basalts. Earth Planet Sci Lett 43:85–92

Masuda A, Nakamura N, Tanaka T (1973) Fine structures of mutually normalized rare earth patterns of chondrites. Geochim Cosmochim Acta 37:239–248

McCulloch MT, Gregory RT, Wasserburg GJ, Taylor Jr HP (1980) A Nd, Sr and O isotopic study of the Cretaceous Samail ophiolite and implications for the petrogenesis and seawater-hydrothermal alteration of oceanic crust. Earth Planet Sci Lett 46:201–211

McCulloch MT, Perfit MR (1981) $^{143}Nd/^{144}Nd$, $^{87}Sr/^{86}Sr$ and trace element constraints on the petrogenesis of Aleutian island arc magmas. Earth Planet Sci Lett 56:167–179

McCulloch MT, Cameron WE (1983) Nd-Sr isotopic study of primitive lavas from the Troodos ophiolite, Cyprus: evidence for a subduction-related setting. Geology 11:727–731

Meijer A (1976) Pb and Sr isotopic data bearing on the origin of volcanic rocks from the Mariana island arc system, Geol Soc Am Bull 87:1358–1369

Melson WG, Vallier TL, Wright TL, Byerly G, Nelsen J (1976) Chemical diversity of abyssal volcanic glass erupted along Pacific, Atlantic and Indian Ocean sea-floor spreading centers. In: The Geophysics of the Pacific Ocean Basin and its Margin. Am Geophys Union Monogr 19:351–367

Miyashiro A (1973) The Troodos ophiolitic complex was probably formed in an island arc. Earth Planet Sci Lett 19:218–224

Moores EM (1982) Origin and emplacement of ophiolites. Rev Geophys Space Phys 20:735–760

Moores EM, Vine FJ (1971) Troodos massif, Cyprus and other ophiolites as oceanic crust: evaluation and implications. Phil Trans R Soc London A268:443–466

Moores EM, Robinson PT, Malpas J, Xenophonotos C (1984) Model for the origin of the Troodos massif, Cyprus, and other mideast ophiolites. Geology 12:500–503

Noiret G, Montigny R, Allègre CJ (1981) Is the Vourinos complex an island arc ophiolite? Earth Planet Sci Lett 56:375–386

O'Nions RK, Hamilton PJ, Evensen NM (1977) Variations in $^{143}Nd/^{144}Nd$ and $^{87}Sr/^{86}Sr$ ratios in oceanic basalts. Earth Planet Sci Lett 34:13–22

Page BM, Suppe J (1981) The Pliocene Lichi melange of Taiwan: its plate tectonic and olistostromal origin. Am J Sci 281:193–227

Pallister JS, Knight RJ (1981) Rare earth element geochemistry of the Samail Ophiolite near Ibra, Oman. J Geophys Res 86:2673–2697

Pearce JA (1982) Trace element characteristics of lavas from destructive plate boundaries. In: Andesites R.S. Thorpe (ed); Wiley Chichester, pp 525–548

Pearce JA, Cann JR (1973) Tectonic setting of basic volcanic rocks determined using trace element analyses. Earth Planet Sci Lett 19:290–300

Pearce JA, Alabaster T, Shelton AW, Searle MP (1981) The Oman ophiolite as a Cretaceous arc-basin complex: evidence and implications. Phil Trans R Soc London A300:299–317

Perfit MR, Gust DA, Bence AE, Arculus RJ, Taylor SR (1980) Chemical characteristics of island arc basalts: implications for mantle sources. Chem Geol 30:227–256

Piepgras DJ, Wasserburg GJ, Dasch EJ (1979) The isotopic composition of Nd in different ocean masses. Earth Planet Sci Lett 45:223–236

Rautenschlein M, Jenner GA, Hertogen J, Hofmann AW, Kerrich R, Schmincke HU, White WM (1985) Isotopic and trace element composition of volcanic glasses from the Akaki Canyon, Cyprus: implications for the origin of the Troodos Ophiolite. Earth Planet Sci Lett (in press)

Robinson PT, Melson WG, O'Hearn T, Schmincke HU (1983) Volcanic glass compositions of the Troodos ophiolite, Cyprus. Geology 11:400–404

Schmincke HU, Rautenschlein M, Robinson PT, Mehegan JM (1983) Troodos extrusive series of Cyprus: a comparison with oceanic crust. Geology 11:405–409

Shido F, Miyashiro A, Ewing M (1971) Crystallization of abyssal tholeiites. Contrib Minerl Petrol 31:251–266

Shih CY, Sun SS, Liou JG, Yen TP, Rhodes JM, Hsu IC (1972) Petrology and geochemistry of the Coastal Range ophiolite of Taiwan. Am Geophys Union Trans 53:535 (abstract)

Spulber SD, Rutherford MJ (1983) The origin of rhyolite and plagiogranite in oceanic crust: an experimental study. J Petrol 24:1–25

Staudigel H, Frey FA, Hart SR (1979) Incompatible trace element geochemistry and $^{87}Sr/^{86}Sr$ in basalts and corresponding glasses and palagonites, Init Rept DSDP 51, 52, 53 (eds T. Donnelly, J. Franchetau et al.) US Govt Printing Office, Washington DC, Vol 2:1137–1143

Stern CR (1979) Open and closed system igneous fractionation within two Chilean ophiolites and the tectonic implication. Contrib Mineral Petrol 68:243–258

Sun SS (1980) Lead isotopic study of young volcanic rocks from mid-ocean ridges, ocean islands and island arcs. Phils Trans R Soc Lond A297:409–445

Sun SS, Nesbitt RW, Sharaskin AY (1979) Geochemical characteristics of mid-ocean ridge basalts. Earth Planet Sci Lett 44:119–138

Suppe J, Liou JG, Ernst WG (1981) Paleogeographic origins of the Miocene East Taiwan Ophiolite. Am J Sci 281:228–246

Tarney J, Saunders AD, Mattey DP, Wood DA, Marsh NG (1981) Geochemical aspects of back-arc spreading in the Scotia Sea and western Pacific. Phil Trans R Soc London A300:263–285

Tatsumoto M (1969) Lead isotopes in volcanic rocks and possible ocean floor thrusting beneath island arcs. Earth Planet Sci Lett 6:369–376

Tatsumoto M (1978) Isotopic composition of lead in oceanic basalts and its implication to mantle evolution. Earth Planet Sci Lett 38:63–87

Tual E, Jahn BM, Bougault H, Joron JL (1985) Geochemistry of basalts from Hole 504B, Leg 83, Costa Rica Rift. Init Rept DSDP, Washington DC, US Govt Printing Office 83:201–214

Vidal Ph, Clauer N (1981) Pb and Sr isotopic systematics of some basalts and sulfides from the East Pacific Rise at 21°N (Project RITA). Earth Planet Sci Lett 55:237–246

Wang Y (1966) Some geologic observations in the Coastal Range, eastern Taiwan. Proc Geol Soc China No. 9:86–93

Wang CS (1976) The Lichi Formation of the Coastal Range and arc-continental collision in eastern Taiwan. Geol Survey Taiwan Bull No. 25:73–86

Wänke H, Baddenhausen H, Spettel B, Teschke F, Quijano-Rico M, Dreibus G, Palme H (1972) The chemistry of Havero ureilite. Meteoritics 7:579–589

White WM (1985) Sources of oceanic basalts: radiogenic isotopic evidence. Geology 13:115–118

White WM, Patchett J (1984) Hf-Nd-Sr isotopes and incompatible element abundances in island arcs: implications for magma origins and crust-mantle evolution. Earth Planet Sci Lett 67:167–185

Whitford DJ (1975) Strontium isotopic studies of the volcanic rocks of the Sunda arc, Indonesia, and their petrogenetic implications. Geochim Cosmochim Acta 39:1287–1302